Implementation and Design of a Fuzzy Power System Stabilizer Using an Adaptive Evolutionary Algorithm

Gi-Hyun Hwang*, Min-Jung Lee*, June-Ho Park and Gil-Jung Kim*****

Abstract - This paper presents the design of a fuzzy power system stabilizer (FPSS) using an adaptive evolutionary algorithm (AEA). AEA consists of genetic algorithm (GA) for a global search capability and evolution strategy (ES) for a local search in an adaptive manner when the present generation evolves into the next generation. AEA is used to optimize the membership functions and scaling factors of the FPSS. To evaluate the usefulness of the FPSS, we applied it to a single-machine infinite bus system (SIBS) and a power system simulator at the Korea Electrotechnology Research Institute. The FPSS displays better control performance than the conventional power system stabilizer (CPSS) for a three-phase fault in heavy load, which is used when tuning FPSS. To show the robustness of the FPSS, it is applied with disturbances such as change of mechanical torque and three-phase fault in nominal and heavy load, etc. The FPSS also demonstrates better robustness than the CPSS. Experimental results indicate that the FPSS has good system damping under various disturbances such as one-line to ground faults, line parameter changes, transformer tap changes, etc.

Keywords: adaptive evolutionary algorithm, fuzzy power system stabilizer, genetic algorithm, evolution strategy

1. Introduction

The research of a power system stabilizer (PSS) for improving the stability of power systems has been conducted as of the late 1960's. Conventionally, a lead-lag controller has been widely used as a PSS. Root locus and Bode plot to determine the coefficient of lead-lag controller [1-6], pole-placement and eigenvalue control [7, 8] and a linear optimal controller theory [9, 10] have been used. These methods, using a model linearlized in the specific operating point, display good control performance in a specific operating point. However, these approaches are difficult to obtain a good control performance in case of operating conditions such as change of load or three phase fault, etc. Therefore, several methods based on adaptive control theory [11, 12] have been proposed to give an adaptive capability to the PSS for nonlinear characteristics of the power system. These methods can improve the dynamic characteristics of power systems, but these approaches cannot be applied for the real time control due to extended execution time.

Recently the research surrounding intelligence control methods such as fuzzy logic controller (FLC) and neural network for the PSS has greatly improved the dynamic characteristics of power systems [13-19]. Fuzzy rules and membership function shape should be adjusted to obtain the best control performance in the FLC. Conventionally, the adjustment is performed by experienced experts or trial and error methods. Therefore, it is difficult to determine suitable membership functions without knowledge of the system. Recently, the evolutionary computation (EC), a type of probabilistic optimal algorithm is employed to adjust the membership functions and fuzzy rules of the FLC. The EC is based on the natural genetics and evolutionary theory. The results of this approach demonstrate fine performance [20-22].

In this paper, we propose an adaptive evolutionary algorithm (AEA). The ratio of population to which the GA and ES will apply is adaptively modified in reproducing according to suitability. The AEA was applied to search the optimal parameters of the membership functions and the suitable gains of the inputs and outputs for the fuzzy power system stabilizer (FPSS). The effectiveness of the FPSS is demonstrated by computer simulation for the single-machine infinite bus system (SIBS) and power system simulator at the Korea Electrotechnology Research Institute. To show the superiority of the FPSS, its performances are compared with those of a conventional power system stabilizer (CPSS).

* Dept. of Electrical and Electronic Engineering, Pusan National University, Korea. (hwanggh@pusan.ac.kr)
* Dept. of Electrical and Electronic Engineering, Pusan National University, Korea.(mnjlee@pusan.ac.kr)
** Dept. of Electrical and Electronic Engineering, Pusan National University, Korea. (parkjh@pusan.ac.kr)
*** Department of Electronics Engineering, Dongseo University
Received February 20, 2003 ; Accepted August 25, 2003

2. Adaptive Evolutionary Algorithm

ES forms a class of optimization techniques motivated by the reproduction of biological systems and the population of individuals evolves towards superior solutions by means of the mutation and selection operation. In this paper, we adopted a (μ, λ)-ES. That is, only the λ offspring generated by mutation competes for survival and the μ parents are completely replaced in each generation. Also, self-adaptive mutation step sizes are used in the ES.

For the AEA to self-adapt its use of GA and ES operators, each individual has an operator code for determining which operator to use. Suppose '0' refers to GA, and '1' to ES. At each generation, if it is more beneficial to utilize the GA, '0's should appear at the end of individuals. If it is more beneficial to utilize the ES, '1's should appear. After reproduction by roulette wheel selection according to the fitness, GA operations (crossover and mutation) are performed on the individuals that have the operator code of '0' and the ES operation (mutation) is performed on the individuals that have an operator code of '1'. Elitism is also used. The best individual in the population then reproduces both the GA population and ES population in the next generation. The major procedures of the AEA are as follows:

1. ***Initialization:*** The initial population is randomly generated. Operator code is randomly initialized for each individual. According to the operator code, GA operations are performed on the individuals with operator code '0', while ES operations are applied where the operator code is '1'.

2. ***Evaluation and Reproduction:*** Using the selection operator, individual chromosomes are selected in proportion to their fitness, which is evaluated by the defined objective function. After reproduction, GA operations are performed on the individuals having an operator code of '0' and the ES operations are performed on the individuals having an operator code '1'. At each generation, the percentages of '1's and '0's in the operator code indicate the performance of GA and ES operators.

3. ***Preservation of Minimum Number of Individuals:*** At each generation, the AEA may fall into a situation where the percentage of the offspring by one operation is nearly 100% and the offspring by another operation dies off. Therefore, it is necessary for the AEA to preserve a certain amount of individuals for each EC operation. In this paper, we randomly changed the operator code of the individuals with a higher percentage until the numbers of individuals for each EC operation became higher than a certain amount of individuals to be preserved. The predetermined minimum number of individuals to be preserved is set to 20% of the population size.

4. ***Genetic Algorithm and Evolution Strategy:*** Real-valued coding is used to represent a solution. Modified simple crossover and uniform mutation are used as genetic operators. The modified simple crossover operator is a way to generate offstrings population, selecting two strings randomly in parent population, as shown in Fig. 1. If crossover occurs in k-th variable, selecting randomly two strings in t-th generation, offstrings of $t+1$-th generation are shown in Fig. 1.

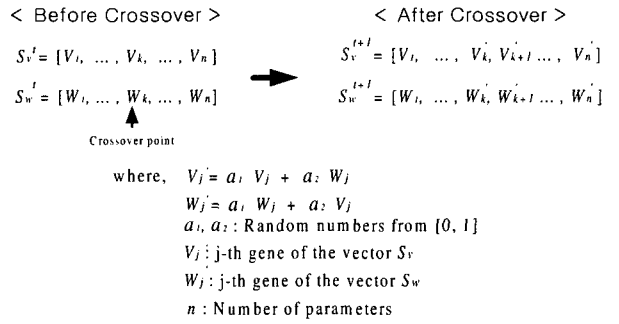

Fig. 1 Modified simple crossover method

In uniform mutation, we selected a random k-th gene in an individual. If an individual and the k-th component of the individual is the selected gene, the resulting individual is as shown in Fig. 2. Only the λ offspring generated by mutation operation competes for survival and the μ parents are completely replaced in each generation. Mutation is then performed independently on each vector element by adding a normally distributed Gaussian random variable with mean zero and standard deviation (σ), as shown in (1). After adapting the mutation operator for ES population, if the improved ratio of individual number is less than δ, standard deviation for the next generation is decreased in proportion to decreased rates of standard deviation (c_d). Otherwise, standard deviation of the next generation is increased in proportion to increased rates of standard deviation (c_i), as shown in (2).

$$v_k^{t+1} = v_k^t + N(0, \sigma^t) \tag{1}$$

$$\sigma^{t+1} = \begin{cases} c_d \times \sigma^t, & \text{if} \quad \phi(t) < \delta \\ c_i \times \sigma^t, & \text{if} \quad \phi(t) > \delta \\ \sigma^t, & \text{if} \quad \phi(t) = \delta \end{cases} \tag{2}$$

5. ***Elitism:*** The finest individual in a population is preserved to perform GA and ES operations in the next generation. This mechanism not only forces the GA not to deteriorate temporarily, but also forces ES to exploit information to guide a subsequent local search in the most promising subspace.

where, $N(0,\sigma')$: Vector of independent Gaussian random variable with mean of zero and standard deviations σ

V_k': k-th variable at t-th generation

$\phi(t)$: Improved ratio of individual number after adapting mutation operator for population of ES in t-th generation

δ: Constants

< Before Mutation > < After Mutation >

$S_i^t = [V_1, \ldots, V_k, \ldots, V_n] \rightarrow S_i^{t+1} = [V_1, \ldots, V_k', V_{k+1}, \ldots, V_n]$

Mutation point

where, V_k': Random value between upper bound and lower bound

Fig. 2 Uniform mutation method

3. Design of Fuzzy Power System Stabilizer Using the AEA

Conventionally, we have used the knowledge of experts and trial and error methods to tune FLC's for a good control performance, but recently many other ways using ECs are proposed to modify fuzzy rule and shape of fuzzy membership function [20-22]. Scaling factors of input/output and parameters of membership function of the FPSS are optimized by means of the AEA using GA and ES adaptively, as described in Chapter 2.

Fig. 3 displays the architecture for tuning scaling factors of input/output and membership function shape of the FPSS using the AEA. As shown in Fig. 3, the rotor speed deviation of generator and the change rate for rotor speed deviation are used as inputs of the FPSS. The control signals of the FPSS are used for enhancing power system damping by supplementary control signals of generators. The FPSS parameters used in this paper are given below.

- Number of input/output variables: 2/1
- Number of input/output membership functions: 7/7
- Fuzzy inference method: max-min method
- Defuzzification method: center of gravity

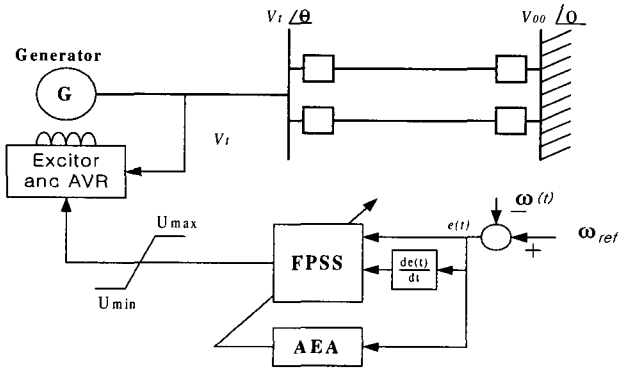

Fig. 3 Configuration for tuning of the FPSS using AEA.

Table 1 Fuzzy rules of proportional-differential type

de / e	NB	NM	NS	ZE	PS	PM	PB
NB	NB	NB	NB	NM	NM	NS	ZE
NM	NB	NB	NM	NM	NS	ZE	PS
NS	NB	NM	NM	NS	ZE	PS	PM
ZE	NM	NM	NS	ZE	PS	PM	PM
PS	NM	NS	ZE	PS	PM	PM	PB
PM	NS	ZE	PS	PM	PM	PB	PB
PB	ZE	PS	PM	PM	PB	PB	PB

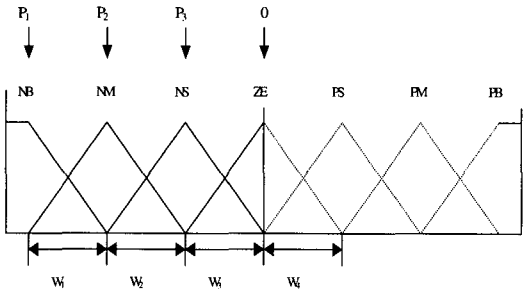

Fig. 4 Symmetrical membership functions

Because deviation and change-of-deviation are used as input variables of the FPSS, proportional-derivative (PD)-like FPSS is used. Rule base for the PD-like FPSS from the two-dimensional phase plane of the system in terms of deviation (e) and change-of-deviation (de) is shown in Table 1. In Table 1, the phase plane is divided into two semi-planes by means of a switching-line. Within the semi-planes, positive and negative control signals are produced, respectively. The magnitude of the control signals depends on the distance of the state vector from the switching line.

When the AEA is tuning the membership functions, fuzzy rules are used for PD-type, as shown in Table 1, where, linguistic variable NB means "Negative Big", NM means "Negative Medium", NS means "Negative Small" and etc. Fig. 4 shows the triangular membership function used in this paper. Because we use 7 fuzzy variables (PB, PM,...,NM, NB) respectively, for input/output of the FPSS, the total membership functions will be 21, so 63 variables that include the center and width of all the membership functions will be adjusted, but it takes a lengthy calculation time to tune 63 variables using the AEA, and suffers from undesirable converging characteristics. In this paper, we fixed the center of ZE to 0 and positive and negative membership functions are constructed symmetrically for 0. Therefore, the number of FPSS parameters will be reduced to 21, which means 3 centers and 4 widths for each variable as shown in Fig. 4.

The flowchart for the design of the FPSS using the proposed AEA is exhibited in Fig. 5. The procedure for the design of the FPSS using the AEA is as follows:

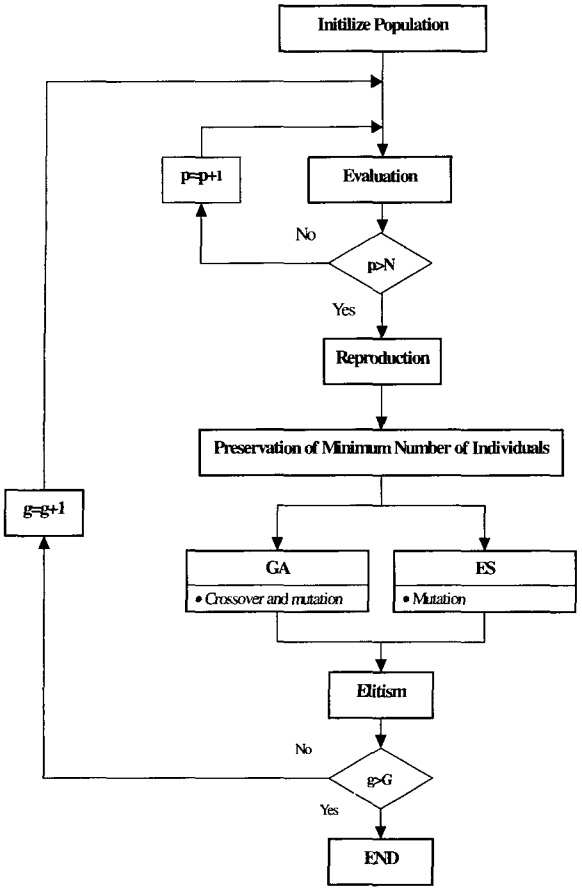

where, P: Number of population
G: Specified generation

Fig. 5 Flowchart for the design of FPSS using AEA

Step 1) Initialize population: Strings are randomly generated between upper bounds and lower bounds of the membership function parameters and scaling factors of the FPSS. The operator code is randomly set to determine whether each string is independent of the GA or ES. The configuration of population is described in Fig. 6. Also scaling factors of the FPSS are tuned by the AEA.

Step 2) Evaluation: Each string generated in Step 1) is evaluated using the fitness function in (3). As shown in (3), the absolute deviation between the rotor speed and the reference rotor speed of the generator is used.

$$Fitness = \frac{1}{1 + \int_{t=0}^{T} | \omega_{ref} - \omega(t) |} \tag{3}$$

where, ω_{ref} : Reference rotor speed of generator
$\omega(t)$: Rotor speed of generator
T : No. of data acquired during specified time

Step 3) Reproduction: We used a roulette wheel to reproduce in proportion to fitness. After reproduction, the individual operator code of '0' is inserted in the population of GA and the individual operator code of '1' is inserted in the population of ES.

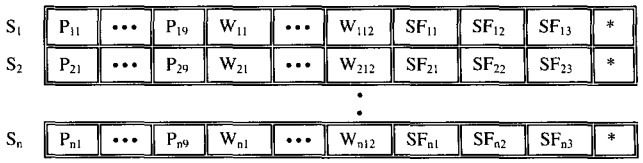

where, n : Population size
P_{ij} : Center of the membership functions
W_{ij} : Width of the membership functions
SF_{ij} : Scaling factors
* : Operator code

Fig. 6 String architecture for tuning membership functions and scaling factors.

Step 4) Preservation of Minimum Number of Individuals: Among the GA and ES, depending on which is stronger, we guarantee a minimum number of individuals having offspring that will disappear by the remaining iterations.

Step 5) GA and ES operation: The individual with an operator code of '0' applies crossover and mutation in GA operators and generates offspring. The individual with an operator code of '1' applies mutation in ES operator and generates offspring.

Step 6) Elitism: We use elitism reproducing the fittest individual to GA and ES population.

Step 7) Convergence criterion: We iterate Step 2) – Step 6) until being satisfied with the specified generation.

4. Case Studies

4.1 Simulation cases of single-machine infinite bus system

We performed nonlinear simulation for the SIBS in Fig. 7 to demonstrate the performance of the proposed FPSS. A machine has been represented by a third order single-axis nonlinear model, as shown in the appendix. Table 2 illustrates the simulation coefficients of the AEA used in the nonlinear simulation. The execution time in PC 586 (300 MHz) takes about 30 minutes to tune the parameters of the FPSS under the conditions in Table 2. Fig. 8 shows the membership function shape of the FPSS tuned by the AEA, where scaling constant of deviation is 0.24, scaling constant of deviation rate is 3.50 and scaling constant of output part is 2.75. We reviewed the performance of the FPSS proposed in this paper and compared it with the CPSS which changes the gain of the PSS through the magnitude of damping constant with the phase compensation method [1]. In the CPSS, time constants (T_1, T_2) were designed based on phase compensation as in (4), where washout filter (T_w) is 3 sec, stabilization gain (K_{pss}) is 7.09, and T_1, T_2

are 0.1 sec and 0.065, sec respectively.

$$V_s = \frac{sT_w}{1+sT_w} K_{pss} \left(\frac{1+sT_1}{1+sT_2} \right) \quad (4)$$

where, Vs: Output of PSS

Fig. 9 (a) shows the fitness values by AEA in each generation. Fig. 9 (b) indicates the number of individuals for GA and ES in the AEA. As shown in Fig. 9, the number of individuals of the GA is higher than that of individuals of the ES in the early generation. But, from generation to generation, the number of individuals of the ES becomes higher than that of individuals of the GA. The AEA produces improved reliability by exploiting the "global" nature of the GA initially as well as the "local" improvement capabilities of the ES from generation to generation.

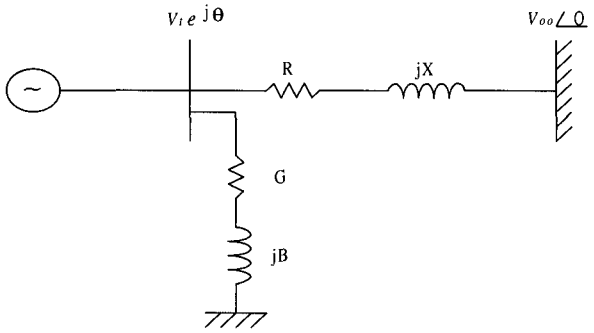

Fig. 7 Single-machine infinite system used in performance evaluation

Table 2 Coefficients for simulation using AEA

Methods	AEA
Size of population	50
Crossover probability	0.95
Mutation probability	0.005
δ	0.5
C_d	0.95
C_1	1.05
C_I	1.05

Analysis conditions used for comparing control performance of the CPSS with the FPSS optimized by AEA are summarized in Table 3. Table 3 is classified into four cases according to the power system simulation cases used in designing the FPSS and in evaluating its robustness. As seen in Table 3, Case-1 is used to design the FPSS and tune scaling constant of input/output variable and membership functions of the FPSS by the AEA. We used Case-2 and Case-4 in evaluating the robustness of the FPSS.

Table 3 Simulation cases used in evaluation of controller performance

Simulation cases	Operating conditions	Disturbance	Fault time [msec]
Case-1	Heavy load P_e = 1.3 [pu] Q_e = 0.015 [pu]	A	40
Case-2		B	-
Case-3	Nominal load P_e = 1.0 [pu] Q_e = 0.015 [pu]	A	40
Case-4		B	-

A: Three phase fault
B: Mechanical torque was changed as 0.1 [pu]

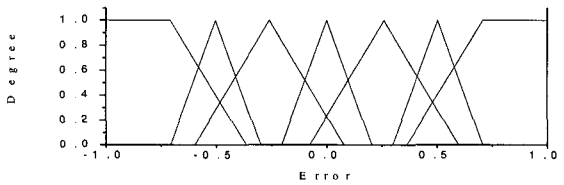

(a) Membership function of deviation

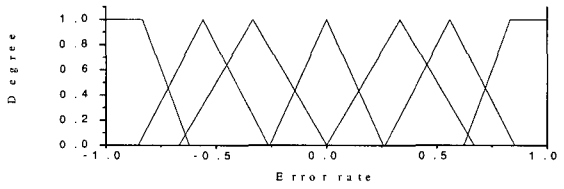

(b) Membership function of change-of-deviation

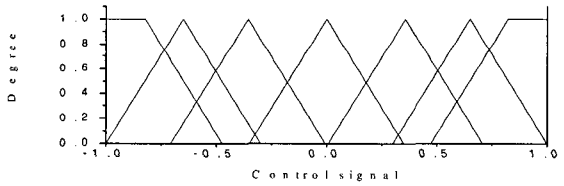

(c) Membership function of output part

Fig. 8 - Tuned membership function of FPSS

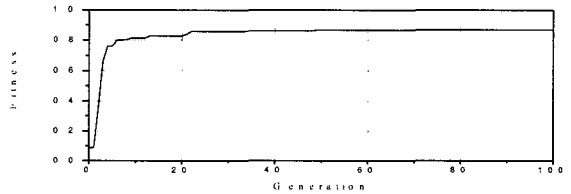

(a) fitness

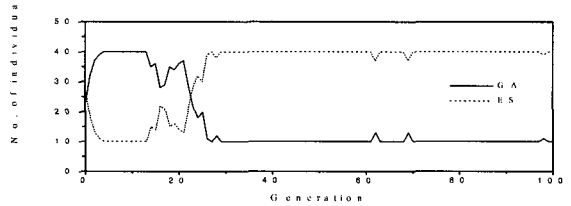

(b) Number of individuals of GA and ES in AEA

Fig. 9 Fitness and number of individuals of GA and ES in each generation

4.1.1 Heavy load condition

Fig. 10 shows generator angular velocity both without the PSS and with the CPSS and FPSS under Case-1 in Table 3. As shown in Fig. 10, the FPSS demonstrates better control performance than the CPSS in terms of settling time and damping effect. To evaluate the robustness of the FPSS, Fig. 11 shows generator response characteristics in case that the PSS is not applied. In this case, the CPSS and the proposed FPSS are applied under Case-2 of Table 3. As shown in Fig. 11, the FPSS shows better control performance than the CPSS in terms of settling time and damping effect.

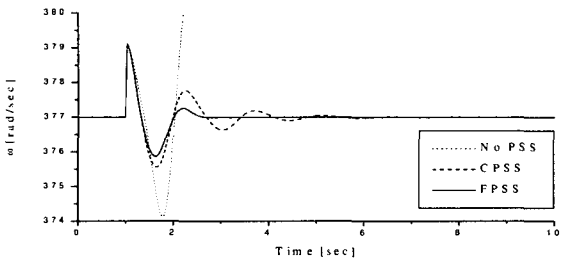

Fig. 10 Responses of generator when three-phase fault was occurred in heavy load

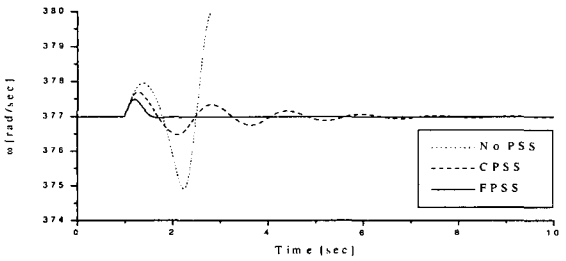

Fig. 11 Responses of generator when mechanical torque was changed to 0.1[pu] in heavy load

4.1.2 Nominal load condition

To evaluate the robustness of the FPSS, Figs. 12-13 show generator response characteristics in case that the PSS is not applied, and the CPSS and proposed FPSS are applied under Cases 3 and 4 of Table 3. As shown in Figs. 12-13, the FPSS shows better control performance than the CPSS in terms of settling time and damping effect.

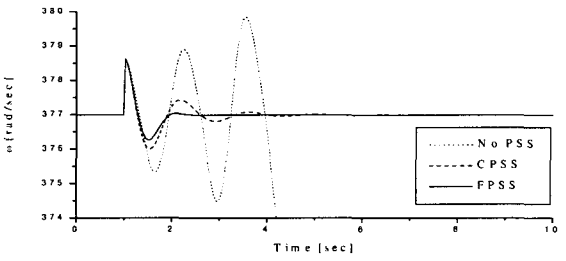

Fig. 12 Responses of generator when three-phase fault was occurred in nominal load

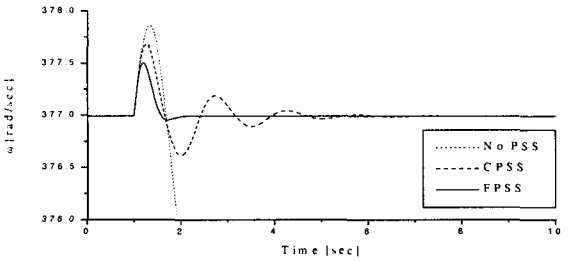

Fig. 13 Responses of generator when mechanical torque was changed to 0.1[pu] in nominal load

4.1.3 Dynamic stability margin [23]

To evaluate the dynamic stability margin of the CPSS and FPSS, a simulation study is conducted with the initial operating conditions of light, nominal and heavy load as given in Table 3. The mechanical torque is increased gradually. The dynamic stability margin is described by the maximum active power in which the system loses synchronism. Table 4 shows the dynamic stability margin. In Table 4, we can find that the FPSS increases the dynamic stability of generator.

Table 4 Dynamic stability margin

Conditions \ Methods		CPSS	FPSS
Light load	Maximum active power [pu]	1.02	1.06
	Maximum generator phase angle [rad]	2.44	2.46
Nominal load	Maximum active power [pu]	1.22	1.27
	Maximum generator phase angle [rad]	2.35	2.45

4.2 Experimental Results

To show the robustness of the proposed FPSS, it has been set up in the power system simulator at the KERI. The configuration of the power system simulator at the KERI is shown in Fig. 14. Part 1 in Fig. 14 is a hardware simulator. It is composed of DC motor-generator set, transmission line simulator, DC motor drive control set and etc. By the use of a PC connected to the microprocessor with A/D, D/A board, angle, terminal voltage and frequency, electrical power output can be measured. In Part 2 of Fig. 14, it is composed of a workstation with A/D, D/A board and main controller for excitation. In this paper, the FPSS tuned by GA is implemented by the workstation of Part II for real time control. Experimental results are saved to the PC in Part 1.

The experiment has been performed subject to the following disturbance: 1) single phase to ground fault 2) impedance of the transmission line changes 3) transformer tap changes 4) electric light changes. When disturbance is sin-

gle phase to ground fault for 0.1 sec., the plot of frequency deviation and electrical power output of the generator are shown in Fig. 15. Suppose impedance of the transmission line increases by sudden loss of one of the transmission lines. The impedance of the transmission line restores 5 seconds following sudden loss. The plot of frequency deviation and electrical power output of the generator are shown in Fig. 16. Fig. 17 shows transformer tap changes of 5% for 5 seconds, plot of frequency deviation and electrical power output of the generator. When the disturbance is a 1.25[Kw] electric light bulb during 2.5 seconds, the plot of frequency deviation and electrical power output of the generator are shown in Fig. 18. As shown in Fig 15 – Fig. 18, the proposed FPSS shows better system damping than that of no PSS.

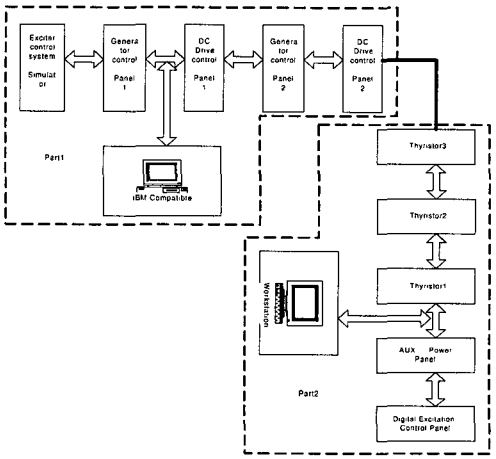

Fig. 14 Configuration of the power system simulator of the KERI

5. Conclusion

In this paper, we tuned membership functions shape and input/output gain of the FPSS using the AEA that is an algorithm having a ratio of population to which the GA and ES will be adaptively modified during reproduction according to fitness. We analyzed simulation results of the FPSS and the CPSS. The results are as follows:

① As a result of applying the AEA to the design of the FPSS, in the early generation, it is shown that the number of population of the GA is higher than that of the population of ES. Also, the number of population of ES grows as the number of generation increases. This indicates that the global search is executed through the GA during early generation and the local search is executed adaptively by means of the ES as the number of generation increases.

② The FPSS displayed better control performance than the CPSS in terms of settling time and damping effect when three-phase fault under heavy load, which is used in tuning the FPSS occurs. To evaluate the robustness of the FPSS, we analyzed dynamic characteristic of the generator for changeable mechanical torque in heavy load, and change of mechanical torque and three-phase fault in nominal load. The FPSS showed superior damping effect to the CPSS.

③ As a result of finding the dynamic stability margin and successive peak damping ratio, the FPSS increased dynamic stability margin to a greater extent and showed the better result than the CPSS in terms of successive peak damping ratio.

④ The FPSS has been set up for power system simulator in the KERI. The performance of the FPSS has been checked subject to various types of disturbances such as single phase to ground fault, impedance of the transmission line changes and transformer tap changes, and all the results indicate the robustness of the proposed FPSS.

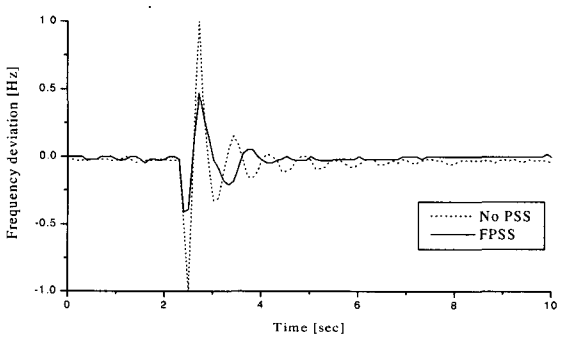

(a) Frequency deviation

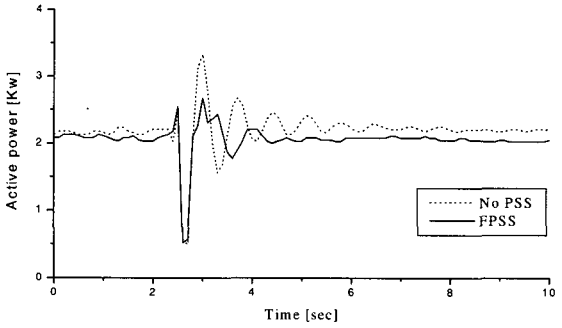

(b) Electrical power output

Fig. 15 Generator responses of one-line to ground fault

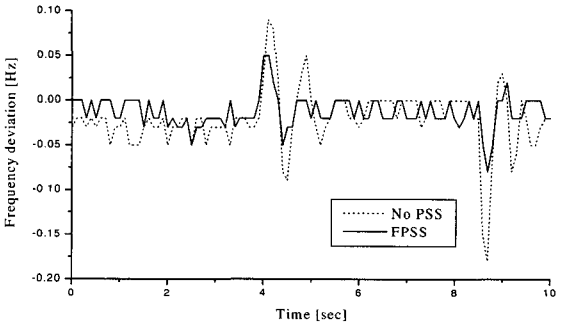

(a) Frequency deviation

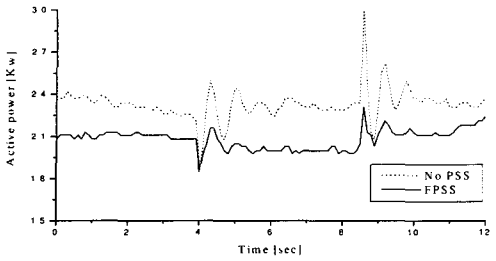

(b) Electrical power output

Fig. 16 Generator response to impedance of the transmission line changes

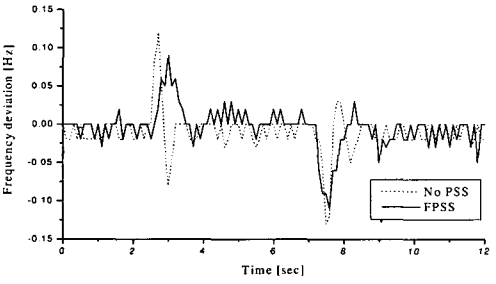

(a) Frequency deviation

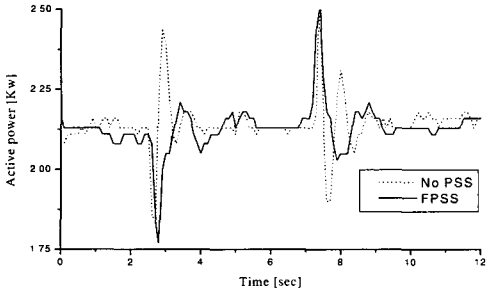

(b) Electrical power output

Fig. 17 Generator responses to transformer tap changes

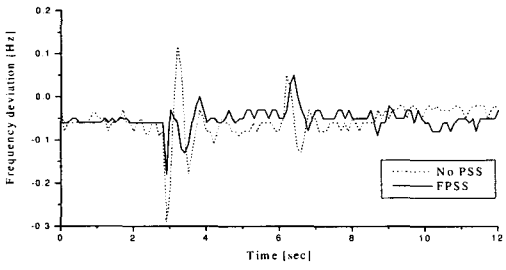

(a) Frequency deviation

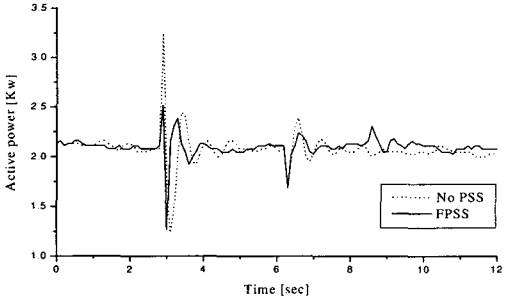

(b) Electrical power output

Fig. 18 Generator responses to electric light changes

Acknowledgements

This work was supported by a grant from the Korea Research Foundation (KRF-2002-003-D00113).

References

[1] Y. N. Yu, Electric Power System Dynamics, *Academic Press*, 1983.

[2] E. V. Larsen and D. A. Swann, "Applying Power System Stabilizers Part I : General Concepts", *IEEE Transactions on Power Apparatus and System*, Vol. PAS-100, No. 6, pp. 3017-3024, June, 1981.

[3] J. Kanniah, O. P. Malik, and G. S.Hope, "Excitation Control of Synchronous Generators Using Adaptive Regulators Part I - Theory and Simulation Result", *IEEE Transactions on Power Apparatus and Systems*, Vol. PAS-103, No. 5, pp. 897-904, May 1984.

[4] H. A. Moussa, M. A. Badr, and A. M. El-Serafi, "Power System Damping Enhancement by Two-axis Supplementary Control of Synchronous Generators", *IEEE Transactions on Power Apparatus and Systems*, Vol. PAS-104, No. 5, pp. 998-1004, May, 1985.

[5] R. Grondin, I. Kamwa, L. Soulieres, J. Potvin, and R. Champagne, "An Approach to PSS Design for Transient Stability Improving Thought Supplementary Damping of the Common Low-Frequency", *IEEE Transactions on Power Systems*, Vol. 8, No. 3, 955-963, August 1993.

[6] C. T. TSE, and S. K. TSO., "Refinement of Conventional PSS Design in Multimachine System by Modal Analysis", *IEEE Transactions on Power Systems*, Vol. 8, No. 2, pp. 598-605, May, 1993.

[7] J. H. Chow and J. J. Sanchez-Gasca, "Pole-Placement Design of Power System Stabilizers` , *IEEE Transactions on Power Systems*, Vol. 4, No. 1, pp. 271-277, Feb., 1989.

[8] D. Ostojic and B. Kovacevic, "On the Eigenvalue Control of Electromechanical Oscillations by Adaptive Power System Stabilizer", *IEEE Transactions on Power Systems*, Vol. 5, No. 4, pp. 1118-1126, Nov., 1990.

[9] R. J. Fleming and Jun Sun, "An Optimal Multivariable Stabilizer for a Multimachine Plant", *IEEE Transactions on Energy Conversion*, Vol. 5, No. 1, pp. 15-22, March, 1990.

[10] C. Mao, O. P. Malik, G. S. Hope, and J. Fun, "An Adaptive Generator Excitation Controller Based on Linear Optimal Control", *IEEE Transactions on Energy Conversion*, Vol. 5, No. 4, pp. 673-678, Dec., 1990.

[11] G. P. Chen, O. P. Malik, G. S. Hope, Y. H. Qin, and G.

Y. Xu, "An Adaptive Power System Stabilizer Based On The Self-Optimization Pole Shifting Control Strategy", *IEEE Transactions on Energy Conversion*, Vol. 8, No. 4, pp. 639-644, Dec., 1993.

[12] T. M. Park and W. Kim., "Discrete-Time Adaptive Sliding Mode Power System Stabilizer with Only Input/Output Measurement", *Electrical Power Energy Systems*, Vol. 18, No. 8, pp, 509-517, 1996.

[13] M. A. M. Hassan, O. P. Malik, and G. S. Hope, "A Fuzzy Logic Based Stabilizer for a Synchronous Machine", *IEEE Transactions on Energy Conversion*, Vol. 6, No. 3, pp. 407-413, Sept., 1991.

[14] M. A. M. Hassan and O. P. Malik, "Implementation and Laboratory Test Results for a Fuzzy Logic Based Self-tuned Power System Stabilizer", *IEEE Transactions on Energy Conversion*, Vol. 8, No. 2, pp. 221-227, June, 1993.

[15] A. Hariri, "A Fuzzy Logic Based Power System Stabilizer with Learning Ability", *IEEE Transactions on Energy Conversion*, Vol. 11, No. 4, pp. 721-726, Dec., 1996.

[16] P. Hoang and K. Tomsovic, "Design and Analysis of an Adaptive Fuzzy Power System Stabilizer", *IEEE Transactions on Energy Conversion*, Vol. 11, No. 2, pp. 455-461, June, 1996.

[17] Y. Zhang, O. P. Malik, G. S. Hope, and G. P. Chen, "Application of an Inverse Input/Output Mapped ANN as a Power System Stabilizer", *IEEE Transactions on Energy Conversion*, Vol. 9, No. 3, pp. 433-439, Sept., 1994.

[18] Y. Zhang, O. P. Malik, and G. P. Chen, "Artificial Neural Network Power System Stabilizers in Multi-Machine Power System Environment", *IEEE Transactions on Energy Conversion*, Vol. 10, No. 1, pp. 147-153, March, 1995.

[19] T. Kobayashi and A. Yokoyama, "An Adaptive Neuro-control System of Synchronous Generator for Power System Stabilization", *IEEE Transactions on Energy Conversion*, Vol. 11, No. 3, pp. 621-627, Sept., 1996.

[20] M. A. Abido and Y. L. Abdel-Magid, "A Genetic-Based Power System Stabilizer", *Electric Machines and Power Systems*, Vol. 26, pp. 559-571, 1998.

[21] M. A. Abido and Y. L. Abdel-Magid, "Hybridizing Rule-Based Power System Stabilizers with Genetic Algorithms", *IEEE Transactions on Power Systems*, Vol. 14, No. 2, pp. 600-607, May, 1999.

[22] M. M. Pedram and H. Seifi, "Extended Algorithm of a Fuzzy-Set Based Power-System Stabilizer with Genetic Algorithm Tuning", *EPEP* Vol. 7, No. 3, pp. 205-210, 1997.

[23] J. He and O. P. Malik, "An Adaptive Power System Stabilizer Based on Recurrent Neural Networks", *IEEE Transactions on Energy Conversion*, Vol. 12, No. 4, pp. 413-418, Dec., 1997.

APPENDIX

A. System Model

$$\frac{dE_q'}{dt} = -\frac{1}{T_{do}'}[E_q' + (X_d - X_d')I_d - E_{fd}]$$

$$\frac{d\delta}{dt} = \omega - \omega_{ref}$$

$$\frac{d\omega}{dt} = \frac{\omega_{ref}}{2H}[T_m - E_q' I_q - (X_q - X_d')I_d I_q]$$

$$\frac{dE_{ef}}{dt} = \frac{K_a}{T_a}(V_{ref} - V_t + V_s) - \frac{1}{Ta}E_{fd}$$

where, $V_t = \sqrt{V_d^2 + V_q^2}$

$$I_d = \frac{1}{\Delta}[\mathrm{Re}(E_d' - V_\infty \sin\delta) + (X_e + X_q')(E_q' - V_\infty \cos\delta)]$$

$$I_q = \frac{1}{\Delta}[\mathrm{Re}(E_q' - V_\infty \cos\delta) - (X_e + X_d')(E_d' - V_\infty \sin\delta)]$$

$$V_d = E_d' + \frac{X_q'}{\Delta}[\mathrm{Re}(E_q' - V_\infty \cos\delta) - (X_e + X_d')(E_d' - V_\infty \sin\delta)]$$

$$V_q = E_q' - \frac{X_d'}{\Delta}[\mathrm{Re}(E_d' - V_\infty \sin\delta) + (X_e + X_q')(E_q' - V_\infty \cos\delta)]$$

$$\Delta = \mathrm{Re}^2 + (X_e + X_d')(X_e + X_q')$$

B. Nomenclature

δ	: Rotor angle of generator
ω	: Rotor speed of generator
ω_{ref}	: Reference rotor speed of generator
H	: Inertia constant of generator
T_m	: Mechanical input of generator
X_d	: d-axis synchronous reactance of generator
X_d'	: d-axis transient reactance of generator
X_q	: q-axis synchronous reactance of generator
E_q'	: q-axis voltage of generator
E_{fd}	: Generator field voltage
T_{do}'	: d-axis transient time constant of generator
I_d	: d-axis current of generator
I_q	: q-axis current of generator
V_t	: Terminal voltage
V_{ref}	: Reference voltage
V_s	: PSS signal
V_{oo}	: Voltage of infinite bus
K_a	: AVR gain
T_a	: Exciter time constant
R_e	: Equivalent resistance of transmission line
X_e	: Equivalent reactance of transmission line

Gi-Hyun Hwang
He received his B.S. degree in Electrical Engineering at Kyungsung University and his M.S. and Ph. D. degrees in Electrical Engineering at Pusan National University. He is currently involved in R&D at the Innotron Corporation. His research interest lies in the applications of intelligent control on power systems.

Min-Jung Lee
He received his B.S. degree in electrical engineering in 1996 from Pukyong National University, Pusan, Korea, and his M.S. and Ph. D. degrees in electrical engineering from Pusan National University, Pusan, Korea, in 1998, and 2001, respectively . He is currently involved in R&D at Innotron Corporation. His research interests are intelligent control, evolutionary algorithms, variable-structure control, adaptive control, and robotics.

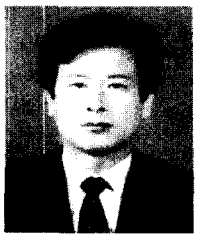

June Ho Park
He received his M.S. and Ph.D. degrees from Seoul National University in Electrical Engineering. He was employed at KERI from 1978 to 1981 and has also been to Penn. State University as a Visiting Scholar. He is currently a Professor at Pusan National University and President of the Research Institute of Computers, Information and Communication.

Gil-Jung Kim
He received his M.S. degree in Electronics Engineering from Dong-A University, Pusan, Korea, in 1981 and his B.S. and Ph.D. degrees in Electronics Engineering from Pusan National University, Pusan, Korea, in 1975 and 1992, respectively. He had been with Kyungnam Junior College from 1978 to 1992, and has also been with the Dept. of Electronics Engineering, Dongseo University, Pusan, Korea as of 1992, where he is an Associate Professor. His research interests include pattern recognition, artificial neural networks, and optical signal processing.